European Journal of Radiology 118 (2019) 130–137

Contents lists available at ScienceDirect

European Journal of Radiology

journal homepage: www.elsevier.com/locate/ejrad

Research article

Impact of acquisition parameters on dose and image quality optimisation in paediatric pelvis radiography—A phantom study

Ali Mohammed Ali[a,*], Peter Hogg[a], Mohamed Abuzaid[b], Andrew England[a]

[a] School of Health Sciences, University of Salford, Salford, M6 6PU, United Kingdom
[b] College of Health Sciences, University of Sharjah, Sharjah, United Arab Emirates

ARTICLE INFO

Keywords:
Pelvis radiography
Paediatric dose reduction
Digital radiography

ABSTRACT

Purpose: Within paediatric pelvis imaging there is a lack of systematic dose optimisation studies which consider age and size variations. This paper presents data from dose optimisation studies using digital radiography and pelvis phantoms representing 1 and 5-year-old children.

Material and method: Dose optimisation included assessments of image quality and radiation dose. Systematic variations using a factorial design for acquisition factors (kVp, mAs, source-detector distance [SDD] and filtration) were undertaken to acquire AP pelvis X-ray images. Perceptual image quality was assessed using a relative and absolute visual grading assessment (VGA) method. Radiation doses were measured by placing a dosimeter at the radiographic centring point on the surface of each phantom. Statistical analyses for determining the optimised parameters included main effects analysis.

Results: Optimised techniques, with diagnostically acceptable image quality, for each paediatric age were: 1-year-old; 65 kVp, 2 mAs and 115 cm SDD, while, 5-year-old; 62 kVp, 8 mAs and 130 cm SDD both included 1 mm Al +0.1 mm Cu additional filtration. The main effect analysis identified situations in which image quality and radiation dose increased or decreased, except for kVp which showed peak image quality when exposure factors were increased. A set of minimum mAs values for producing diagnostic image quality were identified. Increasing SDD, unlike the other exposure factors, showed no trends for producing non-diagnostic images.

Conclusion: The factorial design provided an opportunity to identify suitable acquisition factors. This study provided a method for investigating the combined effect of multiple acquisition parameters on image quality and radiation dose for children.

1. Introduction

The widespread move to digital radiography (DR) has brought additional challenges in balancing image quality with radiation dose. Energy responses of digital detectors are significantly different from film-screen and DR offers greater flexibility in utilising low levels of radiation and when processing the image [1]. While the flexibility from the post-processing of DR images provides the possibility of dose reduction, there have been reports of higher doses through 'dose creep' [2]. Unlike film-screen, if the radiation dose to the image detector is increased the image quality can stay acceptable or even improve [3]. On the other hand, if the dose to the detector decreases the images will start to appear noisy, and observers would observe that image quality has decreased [3]. Thus, there is a need for standardising protocols and exposure parameters in order to remain committed toward the ALARP principle [4]. Previously, a range of studies have highlighted a tendency for operators to overexpose patients instead of underexposing them [2,5]. As a result, several studies have highlighted the need for dose optimisation in DR through determining the appropriate selection of technical parameters [4,6,7].

Researchers [8,9] have used data from hospitals to perform dose optimisation for paediatric pelvis radiography. Some authors have used animal phantoms, such as a lamb's femur to be representative of a 5-year-old child's hip [10]. Others have used test objects for example the CDRAD phantom [11,12] for optimisation studies. Other researchers have used dosimetry phantoms (e.g. ATOM phantoms) to represent the pelvis of children [13–15]. Studies so far have tended to consider only one or two exposure factors and not addressed the combined effects from a wider range of acquisition parameters. Also, previous studies did not consider a factorial approach in order to include the possible effects

* Corresponding author.
E-mail addresses: a.h.m.a.mohammedali@edu.salford.ac.uk (A. Mohammed Ali), P.Hogg@salford.ac.uk (P. Hogg), mabdelfatah@sharjah.ac.ae (M. Abuzaid), A.England@salford.ac.uk (A. England).

https://doi.org/10.1016/j.ejrad.2019.07.014
Received 23 November 2018; Received in revised form 25 May 2019; Accepted 13 July 2019

from a full range of factors exposure parameters, despite this, their contributions are valued but still place further limitations to the current body of knowledge [16,17]. Consequently, our current study seeks to present data from a series of systematic dose optimisation experiments using DR and pelvis phantoms representing 1 and 5-year-old children.

2. Materials and methods

The method included an assessment of visual image quality and radiation dose generated from different combinations of exposure factors. Entrance Surface Air Kerma (ESAK) was considered for dose measurements. Perceptual assessment of pelvic anatomy was conducted as measure for image quality. Main effect analysis of image quality and radiation dose was undertaken for each exposure factor.

2.1. Materials

A series of X-ray exposures were undertaken using a Wolverson Arcoma Arco Ceil general radiography system (Arcoma, Annavägen, Sweden), with a high frequency generator and a VARIAN 130 HS X-ray tube. This system has total filtration of 3 mm Al (inherent 0.5 and added 2.5 mm). A Konica Minolta Aero DR imaging system was used (model CS-7; Aero DR System, Konica Minolta Medical Imaging, USA INC, Wayne, NJ). This comprised of a Cesium Iodide (CsI) detector with a 1,994 × 2,430 pixel matrix, pixel size was 175 µm. Radiation dose measurements were carried out using a solid-state dosimeter (Raysafe X2, Unfors Raysafe AB, Billdal, Sweden). Equipment quality assurance (QA) testing according to the Institute of Physics and Engineering in Medicine (IPEM, 2005) and calibration procedure were performed prior to image acquisition. Tests included assessment of voltage accuracy, exposure time, field size collimation and AEC sensitivity. All QA parameters fell within expected manufacturer tolerances.

Phantoms used in this study were constructed and validated using the method described by Mohammed Ali et al., those phantoms contain simulations for soft tissue and cortical bone [18]. Thus, the visual contrast within human pelvis can be evaluated within these phantoms, since the key imaging priority is associated with the perception of subjective contrast from the bony structures and their margins [19]. The AP thicknesses of the phantoms were 9 cm and 12 cm for the ages 1 and 5-year-old, respectively.

Two 5 mega-pixel monochrome liquid crystal (LCD) monitors DOME E5 (by NDSsi, Santa Rosa, ca) were used in this investigation to display the acquired images (Native resolution; 2560 × 2048), and RadiForce GS251 (21.3 inch). Each monitor self-calibrates to the standard grey scale once it is turned on. The Digital Imaging and Communications in Medicine (DICOM) grey scale standard display function (GSDF) was used, with a luminance of > 400 cd/m2 (according to the National Electrical Manufacturers Association, 2006). In addition, ambient light was dimmed to a level simulating clinical image evaluations, approximately 30 lx.

2.2. Methods

2.2.1. Data collection

Literature identified that a factorial study design would be the most appropriate method for studying the effect from a number of different acquisition factors [16,20]. Benefits of a factorial design allows the estimation of the effects of a single factor with the influence of several other factors and generally this results in more valid conclusions in comparison to several experiments which attempt to perform investigations with a single factor study [16,17]. The exposure factor combinations were used to acquire AP pelvis images using 1 and 5-year-old pelvis phantoms. For each phantom, the total number of images according to the factorial study design [17] were calculated according to the equation below:

$$N = K_1 \text{ X } K_2 \text{ X } K_3 \text{ X } K_4 \quad (1)$$

Where K_{1-4} represents the number of increments within each exposure factor.

Acquisition parameters were as follows. For the 1-year-old phantom 50–80 kVp (3 kVp increments) and 1–12 mA s (1 mAs increments); for the 5-year-old phantom 56–89 kVp (3 kVp increments) and 1–16 mA s (1 mAs increments), both at 100–145 cm source-detector distance (SDD) (15 cm increments) and inherent filtration (zero, 2 mm Al and 1 mm Al + 0.1 mm Cu). This resulted in 1584 images being generated for the 1 year old and 2016 images for the 5-year-old. All the images were produced using a fine focal spot (head toward the anode orientation) and paediatric hip/pelvis post-processing algorithm.

2.2.2. Radiation dose

The Raysafe X2 dosimeter was positioned on the surface of each phantom at the centre of the X-ray field. Entrance Surface Air Kerma (ESAK) measurements were conducted for each exposure factor combination for the 1 and 5 years-old phantoms. Each measurement was repeated three times and the corresponding mean was recorded.

2.2.3. Image quality evaluation

Visual image quality evaluations were performed in two phases.

The first phase included an assessment of sharpness and noise of bony anatomy (femoral heads, femoral epiphysis, pubic bones, ischium, sacro-iliac joints, femoral necks, sacrum, L5 vertebral body and iliac crests), in addition, the sharpness of the bony cortex and bony trabecula pattern appearance on a chicken bone was included in the sharpness score.

Visual image appraisal was performed using relative visual grading assessment (VGA) [21] as the first phase, where all experimental images were randomly displayed in DICOM format. The reference image, within this phase, was chosen by a group including two experienced radiographers. Using the sharpness and noise of bony anatomy aforementioned in this section, the reference image was chosen to be at an intermediate visual image quality level in order to allow the full use of the image quality scale. The ICC score for the observer was measured against the mean score of sharpness and noise of five experienced (> 5-year post-qualification) radiographers. Thus, reliability data can confirm that the lead researcher can perform the assessment of image quality during the first phase. The interpretation of ICC score is as follows; poor (0–0.2), fair (0.21–0.4), moderate (0.41–0.6), excellent (0.61–0.8) and almost perfect (0.81–1) [22], other interpretations considers that an ICC score of more than 0.75 is excellent agreement [23]. The observer evaluated the first phase of visual image quality using a 3-point Likert scale and was able to decide whether the sharpness level and noise level of specific regions of interest (pelvic bony anatomies) and the overall image quality were: worse (2), equal to (3), or better (4), than that of the reference image. The net image quality score (IQ (sharpness & clarity)) was calculated by averaging the mean sharpness and the mean clarity (opposite of noise).

The second phase of the visual image quality evaluation included sampling, from each phantom, 84 images that contained a range of image quality levels found within the first phase to be scored using a binary scale. The 84 X-ray images chosen were of different visual image quality levels; ranging from the lowest to the highest according to the visual scale. The largest proportion (of the number of images out of the sample) of visual image quality scores represented the intermediate level of image quality. Where the higher and lower visual image quality score were around 5 images each, the rest were distributed over the middle (intermediate) levels. This distribution provided the opportunity for observers to score more images from the levels of image quality which would have the lowest consensus. Therefore, more robust decisions on diagnostic image quality can be derived from this work.

The 84 images, from each age, were displayed to two consultant radiologists, each with more than 30 years clinical experience, and

were invited to indicate whether an image had adequate diagnostic quality or not (Yes/No). Thus, the image quality level with diagnostic quality was identified; this level was used to determine the exposure factor combinations that produced an acceptable level of image quality within the first phase of the evaluation.

2.2.4. Data analysis

Comparisons were conducted between exposure factor combinations in terms of lowest radiation dose and diagnostic acceptability of image quality. Thus, the five lowest radiation dose exposure techniques which produced acceptable image quality were identified. A main effect analysis was conducted for each exposure factor in order to investigate the trend on image quality and radiation dose when increasing each exposure factor. The main effect output is a graphical plot of dependent variable means against the various levels of each exposure factor increments. Statistical analysis was conducted in SPSS software version 23 (IBM corp., Armonk, NY, USA). A Friedman test was considered for non-parametric repeated measure data, it was performed after testing the data distribution using the Shapiro-Wilko test. P values > 0.05 were considered indicative of an approximately normally distributed dataset.

3. Results

The image quality was assessed by an observer with a reliable intra-class correlation (ICC) score; sharpness: 0.757 (95% CI 0.731–0.889) and noise: 0.847 (95% CI 0.886–0.963). These high levels of agreement provide evidence that the lead observer can perform visual image quality assessments in the first phase.

3.1. Optimum technique

3.1.1. 1-year-old

The five optimum (lowest dose) exposure factors are listed in Table 1. The optimum (lowest dose) exposure factor combinations were 53, 59 and 65 kVp; 1 mm Al +0.1 mm Cu additional filtration and resulted in radiation doses ranging from 15.31 to 25.9 μGy. The exposure factors producing the lowest dose was 65 kVp, 2 mAs and 115 cm SDD. The acceptable image quality with the lowest dose for the 1-year-old phantom is illustrated in Fig. 1.

3.1.2. 5-year-old

The five optimum (lowest dose) exposure factors are listed in Table 2. The lowest radiation doses were 56, 59, 62 and 74 kVp; 1 mm Al +0.1 mm Cu additional filtration and resulted in radiation doses ranging from 42.9 to 49.12 μGy. The lowest dose exposure factor combination was 62 kVp, 8 mAs and 130 cm SDD. See Fig. 2, which represents the acceptable image quality with the lowest radiation dose for the 5-year-old phantom.

Friedman tests, for both phantoms, showed that SDD and additional filtration had statistically significant effects on image quality and radiation dose ($p < 0.05$). Also, the main effect analysis showed that kVp and mAs had significant effects on image quality and radiation dose.

Table 1
Exposure factors (1-year old) that produced the five lowest dose acceptable quality images.

Optimum exposure factors: 1 year old						
Rank	KVp	mAs	SDD (cm)	Filter (mm)	ESAK (μGy)	DAP (mGy cm^2)
1	65	2	115	1 Al + 0.1 Cu	15.31	4
2	65	5	145	1 Al + 0.1 Cu	23.93	7
3	53	7.1	145	2 AL	24.64	7
4	59	6.3	130	1 Al + 0.1 Cu	25.68	8
5	59	8	145	1 Al + 0.1 Cu	25.9	8

3.2. Main effect

The main effect plots for image quality when increasing each exposure factor are presented in Figs. 3–5, each figure contains three plots representing three different levels of additional filtration. The radiation dose showed a continuous increase with increasing kVp and mAs and a continuous decrease when increasing SDD. The horizontal line on each plot represents the diagnostically acceptable image quality level determined by the two radiologists. The main effect plots showed, for both paediatric ages, that the additional filtration combination of 0.1 mm Cu +1 mm Al had the highest effect on reducing image quality and radiation dose and the next was 2 mm Al filtration and the last was zero additional filtration.

For the 1-year-old, image quality increased as kVp increased until 59–65 kVp, which represented the point of saturation (Fig. 3a–c), this was followed by a fall in image quality. This behaviour was seen for zero and 2 mm Al additional filtration. For the compound filtration with the 1-year-old, there was a relatively small increase in image quality as kVp increased to 59 kVp, where saturation occurred. The image quality for zero filtration and 2 mm Al was above the diagnostically acceptable level (Fig. 3a & b). While, for the compound filtration, the image quality was under the diagnostically acceptable level at lower tube potentials (50 and 53 kVp only; Fig. 3c). For the 5-year-old, increasing tube potential caused a slight reduction (between 68 and 71 kVp) in image quality at zero filtration, for the other filtration levels, saturation started at 65 kVp (Fig. 3d–f).

Within the 1 and 5 year-old optimisation studies, the main effect analysis showed continuous increase in image quality as mAs increased (Fig. 4). Within 1-year-old study, the minimum mAs values for obtaining diagnostic image quality were 2.8, 4 and 5 for 0, 2 mm Al and 0.1 mm Cu +1 mm Al, respectively (Fig. 4a–c). For the 5-year-old, the mAs values needed to increase by 1 mAs increment more than mAs for the 1-year-old phantom to achieve acceptable image quality (Fig. 4d–f).

The main effect analysis showed a continuous decrease in image quality as SDD increased for 1 and 5-year-olds. However, the increase in SDD did not reduce image quality lower than the diagnostic acceptable level for either ages (Fig. 5).

4. Discussion

4.1. Optimised exposure technique

4.1.1. kVp

With respect to kVp, the most important function of tube potential is to provide at least partial penetration through all tissues that need to be demonstrated [24]. Increasing the kVp increases the average energy and the intensity of the X-ray beam [25]. Dose optimised images for the 1-year old, which produced the lowest doses with acceptable image quality, used 53, 59 and 65 kVp (Table 1). The 5-year-old optimisation study showed that the lowest five radiation doses used 56, 59, 62 and 74 kVp (Table 2). This kVp range is higher on average than the kVp range from 1-year-old optimisation study and represents the thicker body part when comparing 1 and 5-year-olds. These results are in broad agreement with the literature and supports the need for higher kVp ranges for thicker body parts in paediatric imaging [26].

When comparing with the literature, a DR study found 55 and 90 kVp together with 0.3 mm Cu filtration as the dose optimised exposure technique for 1 and 5-year-old children, respectively [14]. Another study found 50 kVp, 5 mAs and 0.1 mm Cu filtration for 5-year-old children with computed radiography (CR) [13]. The difference in results from our current study when compared to the aforementioned studies could relate to the limited exposure factors (i.e. SDD and filtration) used. In addition, the researchers used dosimetry phantoms which may limit their findings as these phantoms were based on average bone density (cortical and trabecular bone) to simulate bone tissue [27], while trabecular bone, with a higher density, exists within

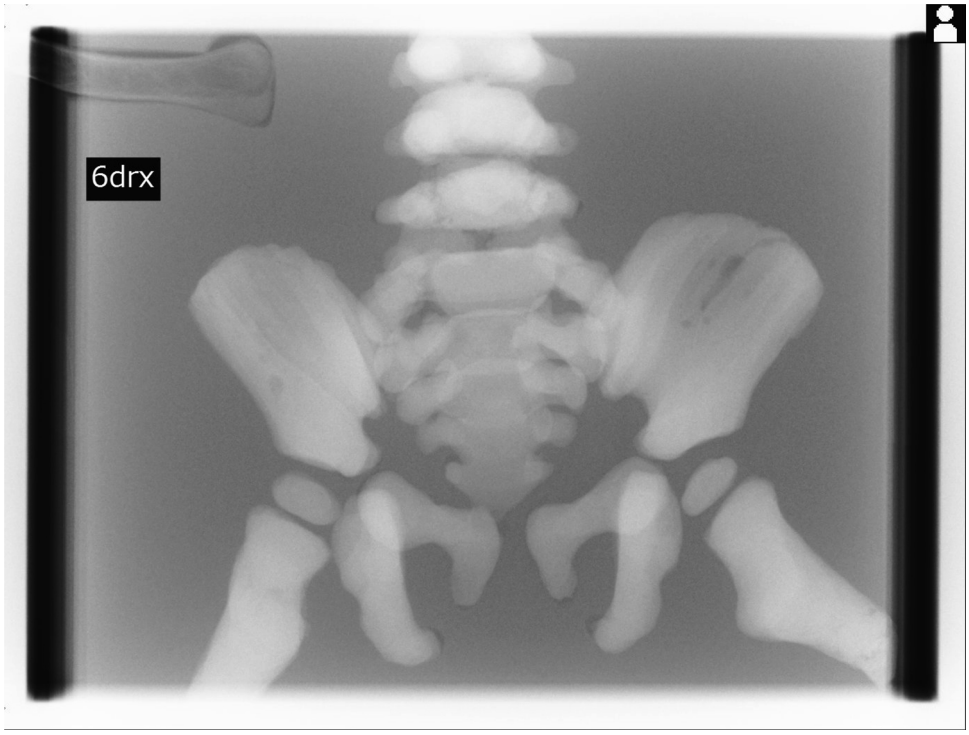

Fig. 1. The acceptable image quality with the lowest radiation dose for the 1-year-old phantom.

Table 2
Exposure factors (5-years old) that produced the five lowest dose acceptable quality images.

	Optimum exposure factors: 5 year old					
Rank	KVp	mAs	SDD (cm)	Filter (mm)	ESAK (μGy)	DAP (mGy cm^2)
1	62	8	130	1 Al + 0.1 Cu	42.95	14
2	59	10	130	1 Al + 0.1 Cu	44.17	14
3	56	16	145	1 Al + 0.1 Cu	45.38	15
4	59	14	145	1 Al + 0.1 Cu	48.27	16
5	74	5	130	1 Al + 0.1 Cu	49.12	15

the human pelvis. Thus, the lower densities of simulated bone within dosimetry phantoms could be the reason for observing greater visibility at lower tube potentials in order to compensate for the underestimated bone contrast within dosimetry phantoms.

4.1.2. mAs

The range of mAs values for the 1-year-old (2–7.1 mA s) that produced diagnostic images were lower when compared to the 5-year-old (5–16 mA s) (see Tables 1 and 2). This relates to the corresponding thickness of the 5-year-old phantom and the amount of radiation reaching the DR imaging detector. As a result, higher radiation intensity for thicker body parts are required to reach the image receptor and to achieve a sufficient signal when compared to noise in order to carry sufficient anatomical information [24]. This can explain the differences in mAs when achieving sufficient image quality for diagnosis between phantoms. When compared to the mAs values for the 1-year-old optimisation study, the higher mAs (˜40%) for the 5-year-old can be attributed to the thicker body part associated with their ages.

Compared to the literature, the lowest mAs associated with acceptable image quality was (1-year-old; 2 mAs and 5-year-old; 5 mAs) which were lower than 6.3 mAs and 60 kVp (5.2 mm Al) found in a study using a lamb's femur to represent a 5-year-old child's hip [10]. The difference in mAs can be related to the size differences between the 1 and 5-year-old pelvis phantom, which are thinner than the lamb's hip (20 cm), which would require a lower mAs, in addition to the difference in the applied filtration and kVp [28].

4.1.3. SDD

The optimised techniques showed images with acceptable image quality and lowest doses appeared at large SDDs (1-year-old; 130 and 145 cm, 5-year-old; 115, 130 and 145 cm; Tables 1 and 2). This can be linked to the advantage of increasing SDD during imaging which reduces the radiation dose to the patient, reduces the penumbra in the image thereby increasing image sharpness. A larger SDD also results in less image magnification [24]. The 1 and 5-year-old optimisation studies showed that SDD had a significant effect in reducing image quality and radiation dose (Friedman test). In addition, images with diagnostically acceptable quality and lower doses appeared at SDDs of 115, 130 and 145 cm. There is one point to consider regarding the 145 cm SDD, it must be noted that this distance may not be available with all X-ray machines and as such optimisation processes would need to consider alternatives. It is also possible that depending on the individual X-ray unit other features may be present or absence which could affect the parameters available for dose optimisation. We believe that in this study we have fully tested a range of commonly available acquisition parameters.

Karami et al. used clinical data to investigate SDD when optimising CR imaging systems (paediatric CXR) [29]. Their study found that the increased SDD from 100 to 130 cm reduced the radiation dose significantly with no significant effect on image quality ($P > 0.05$). Despite the similarity in dose reduction to this study, there are differences in the impact of SDD changes on image quality (not significant), while SDD within this report showed a significant effect for the 1-year-old phantom (diagnostic image quality). The non-significant effect of SDD on image quality from the study by Karami et al. could be related to the variations in patient's size and exposure factors that usually exist in hospital studies, these could have a major impact on the image quality and radiation dose outcomes [30].

4.1.4. Additional filtration

With regards to additional filtration, the acceptable images with the

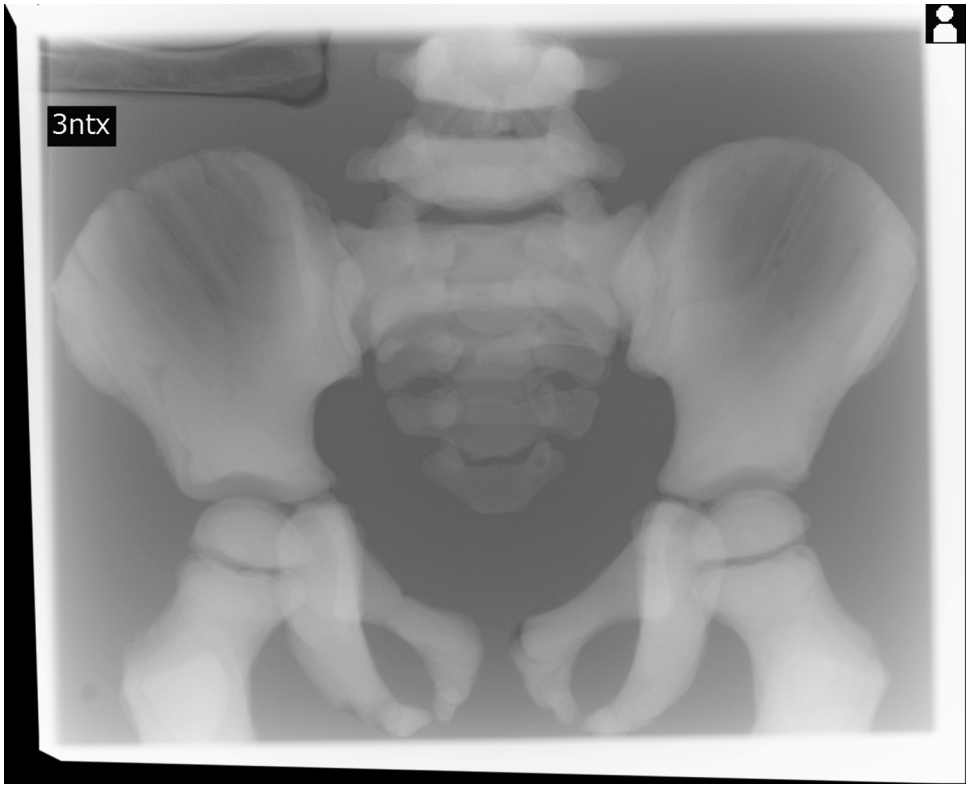

Fig. 2. The acceptable image quality with the lowest radiation dose for the 5-year-old phantom.

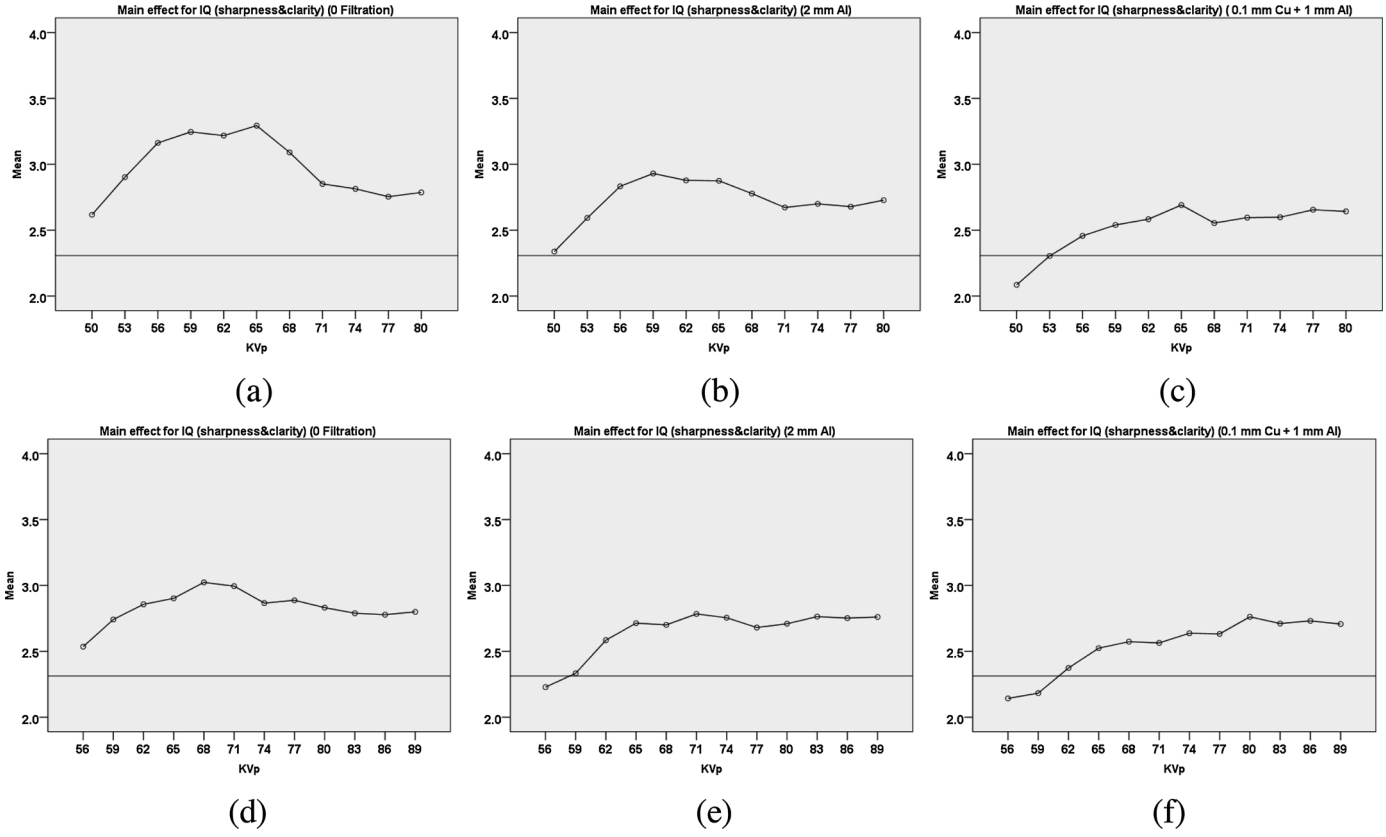

Fig. 3. 1-year-old (A–C) and 5-year-old (D–F) main effect plots for image quality when increasing the kVp; (A & D) zero filtration; (B & E) at 2 mm Al and (C & F) at 0.1 mm Cu +1 mm Al.

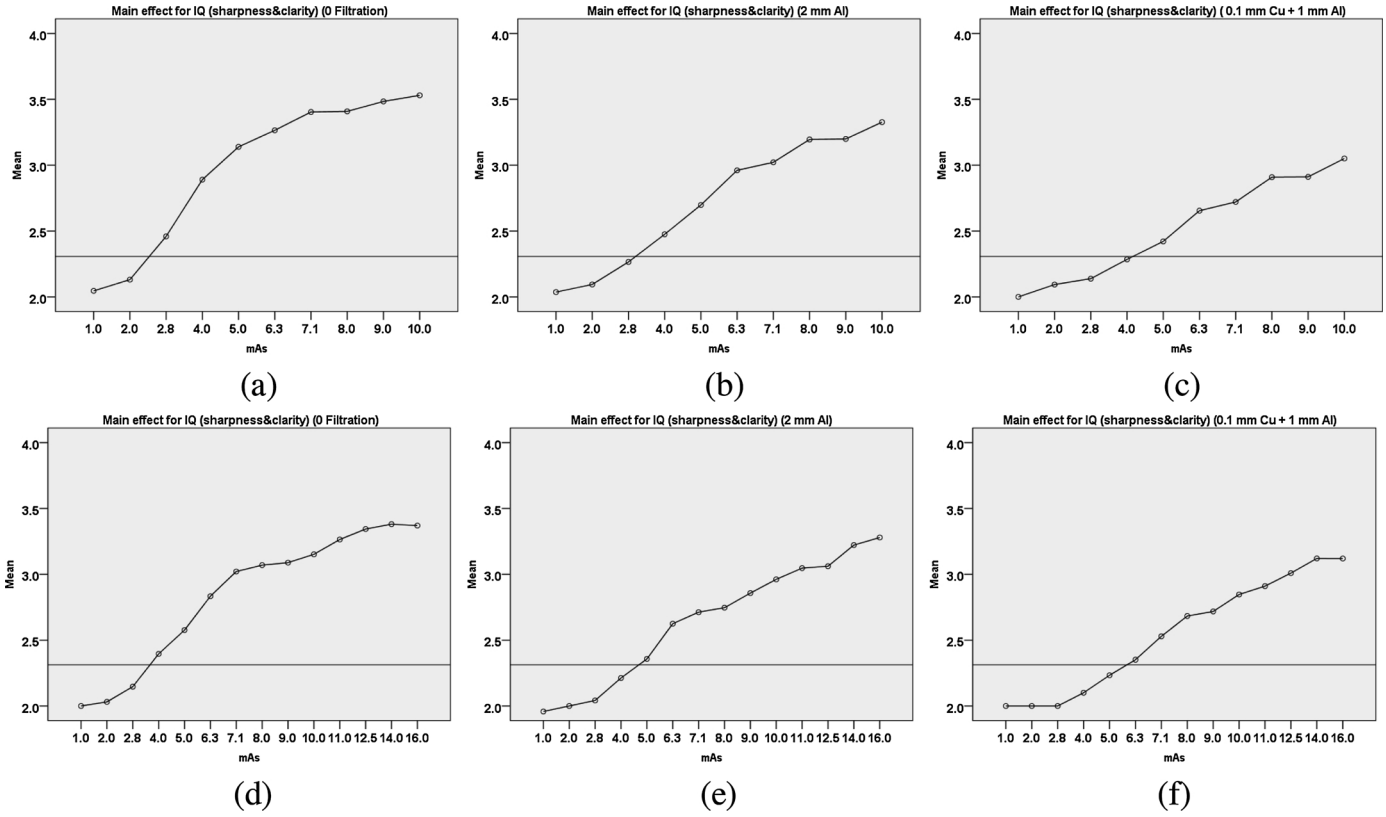

Fig. 4. 1-year-old (A–C) and 5-year-old (D–F) main effect plots for image quality when increasing the mAs; (A & D) at zero filtration, (B & E) at 2 mm Al, (C & F) at 0.1 mm Cu + 1 mm Al.

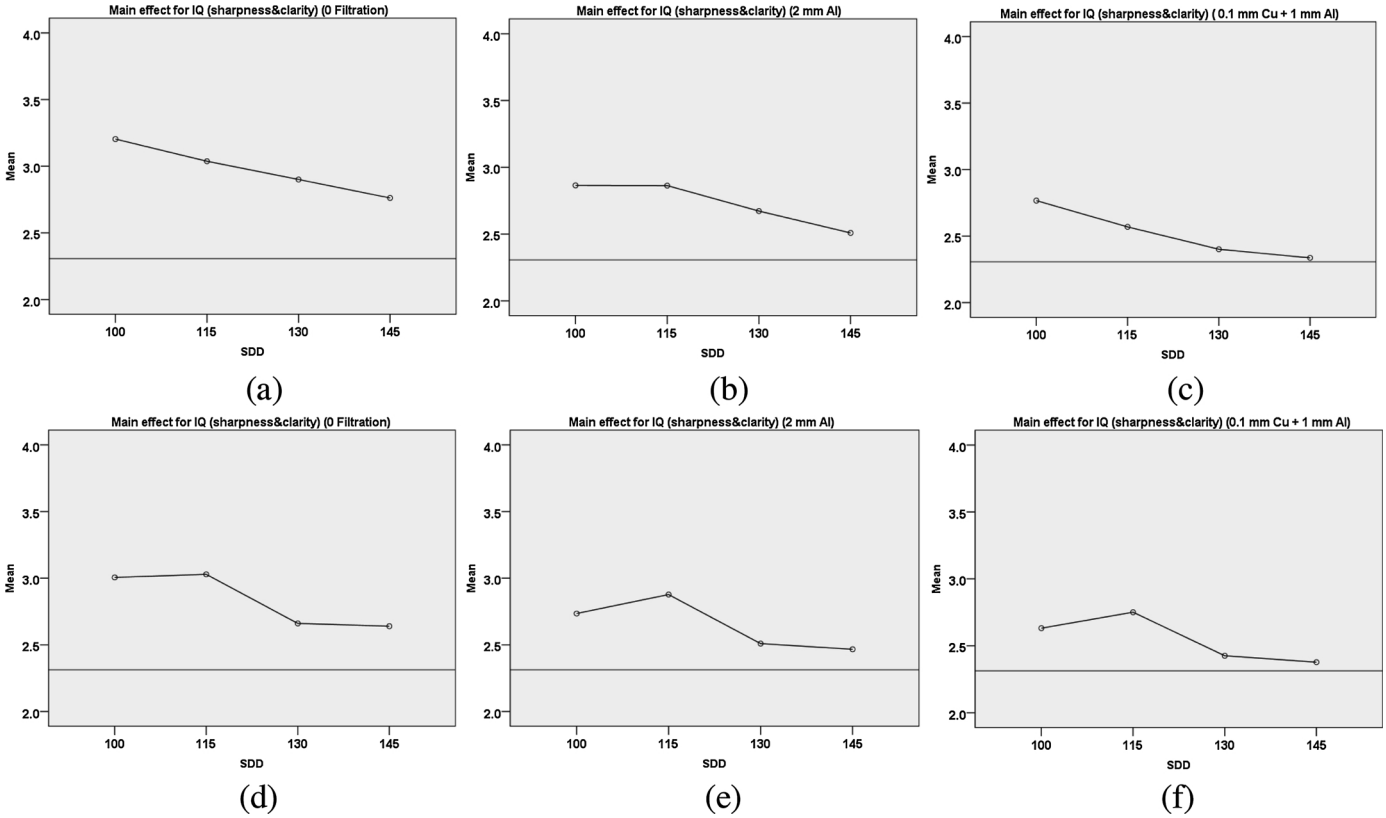

Fig. 5. 1-year-old (A–C) and 5-year-old (D–F) main effect plots for image quality when increasing the SDD; (A & D) at zero filtration, (B & E) at 2 mm Al, (C & F) at 0.1 mm Cu + 1 mm Al.

lowest dose in the 1 and 5-year-old optimisation studies (1-year-old; 15.31 μGy and 5-year-old; 42.95 μGy, see Tables 1 and 2) were almost all with 1 mm Al + 0.1 mm Cu of additional filtration. This can be explained by the ability of filtration to remove lower energy X-ray photons and, hence, reduce the radiation dose [25].

Additional filtration, as determined by the Friedman test, showed a significant effect on radiation dose and image quality, this can be related to the reduction in the amount of X-ray photons reaching the image detector along with increasing beam average energy [25], both would decrease image quality and radiation dose. Similar results were found by Brosi et al, who found significant differences in image quality and the radiation dose for AP paediatric pelvis radiography [11].

Other studies agreed with our results in that statistically significant effects from filtration were for radiation dose only, while they disagreed with our work demonstrating no significant effect on image quality by applying extra filtration [14,15,31]. There are some methodological differences which could explain the difference in results, for example filtration levels, kVp ranges and limitations in the imaging phantoms used. For example, they used either test objects or ATOM dosimetry phantoms, both phantom types have limitations in representing bony anatomical shape or tissue, respectively [27,32].

4.2. Main effect

Linking the main effect analysis for 1 and 5-year-old phantoms (Fig. 3) with kVp trends, there was an increase in image quality until a plateauing point at specific kVp values (1-year-old; 59 kVp and 5-year-old: 65 kVp at zero filtration then depending on the level of filtration), after which the mean diagnostic image quality generally started decreasing. This implies that image quality can be at its highest level within the 59–65 and 65–77 kVp for 1 and 5-year-olds, respectively. This response can be explained by the k-edge related to the materials of the DR detector, which showed that there is a specific energy range that has the maximum X-ray absorption [7]. The added filtration, as appeared in main effect plots (Figs. 3 and 4), showed reduction in image quality but not under the level of diagnostic acceptability, except for cases at low tube potentials. In connecting this with producing the lowest dose, the literature demonstrates that using a higher kVp with lower mAs is a dose reduction imaging technique [33], in addition, to using additional filtration (1 mm Al with 0.1 or 0.2 mm Cu) [26,34]. Thus, the use of the aforementioned kVp ranges with additional filtration (1 mm Al + 0.1 mm Cu) can achieve the best dose to image quality interplay.

The continuous trends of image quality and radiation dose via increasing mAs, SDD and filtration (as shown in Figs. 4 and 5) can be explained by the relationship with the quantity of x-ray photons reaching the patient and the associated signal to noise ratio reaching the image detector [25]. There were minimum values for mAs that showed diagnostically acceptable image quality at each filtration level for each age (1-year-old; 2.8 mAs and 5-year-old; 4 mAs at zero filtration then these values increase with additional filtration). This can be interpreted in clinical practice as the minimum mAs required for each age and at each filtration level.

For the 1 and 5-year-old phantom images, the continuous decrease in image quality with increasing SDD resulted in images still being diagnostically acceptable level. With more added filtration, the decrease in image quality reached closer, but still above, the minimum diagnostic quality level (Fig. 5). This means that using higher SDD can be promising for optimisation in clinical practice as it still produces images with diagnostic quality at a reduced dose. One point to mention is the effect of magnification was not considered in this study. It is possible to measure the decrease in the dimensions of the bony anatomy when the SDD was increased. This would warrant further study and, in our case, there was a significant effect (from the Friedman test data) on image quality when increasing the SDD.

Similarity trends were found in literature in a hospital study by Martin et al. [8]. They found, for manual exposures, an increase in visual image quality when increasing kVp. Similar results were found in the literature from a study investigating AP projections of the wrist and ribs in children. The study by Martin et al. [8], demonstrated an increase in image quality (including contrast, sharpness and noise) and radiation dose (ESD) when increasing mAs [35]. Regarding the effect of SDD reported in the literature when using the AEC, similar results were found by Tugwell et al. and Mraity who showed that increasing the SDD caused a decrease in ED [36,37]. Also, the image quality showed similar response to report by Mraity who found a decrease in perceptual image quality when SDD was increased [37].

5. Conclusion

For a 1-year-old AP pelvis, based on the experiments within this study, the recommended acquisition parameters are 65 kVp, 2 mAs, 115 cm SDD and 1 mm Al + 0.1 mm Cu filtration. For a 5-year-old, the dose optimised exposure factors are 62 kVp, 8 mAs, 130 cm SDD and 1 mm Al + 0.1 mm Cu filtration. A universal recommendation from our study is for the two ages, that the use of additional filtration (1 mm Al + 0.1 mm Cu) is recommended.

Main effect analysis showed that a continuous increase of exposure factors would yield a continuous increase/decrease in radiation dose and image quality. However, unlike, the other exposure parameters, the kVp showed plateauing effect or an effective kVp range (59–65 and 65–77 kVp for 1 and 5 year olds, respectively). There were minimum mAs values found within each paediatric age and at each filtration level that could produce diagnostic image quality (Fig. 4). The increase in SDD (from 100 to 145 cm) showed no obvious trends when considering the diagnostic image quality range. Finally, a factorial study design showed the ability to undertake a comprehensive dose optimisation study evaluating multiple acquisition factor effects at the same time. It, also, help provide a full understanding for the influence of each factor on image quality and radiation dose. A greater number of factorial study designs, for systematic dose optimisation studies, are warranted.

References

[1] E. Vaño, J.M. Fernández, J.I. Ten, C. Prieto, L. González, R. Rodríguez, H. de Las, Heras, Transition from screen-film to digital radiography: evolution of patient radiation doses at projection radiography, Radiology 243 (2007) 461–466, https://doi.org/10.1148/radiol.2432050930.
[2] T. Herrmann, T.L. Fauber, J. Gill, C. Hoffman, D.K. Orth, P. a Peterson, R.R. Prouty, A.P. Woodward, T.G. Odle, Best practices in digital radiography, Radiol. Technol. 84 (2012) 83–89 doi:84/1/83 [pii].
[3] K. Al Khalifah, A. Brindhaban, Comparison between conventional radiography and digital radiography for various kVp and mAs settings using a pelvic phantom, Radiography 10 (2004) 119–125, https://doi.org/10.1016/j.radi.2004.02.006.
[4] S. Mc Fadden, T. Roding, G. de Vries, M. Benwell, H. Bijwaard, J. Scheurleer, Digital imaging and radiographic practise in diagnostic radiography: an overview of current knowledge and practice in Europe, Radiography (2017) 8–12, https://doi.org/10.1016/j.radi.2017.11.004.
[5] D. Gibson, R. Davidson, Exposure creep in computed radiography, Acad. Radiol. 19 (2012) 458–462, https://doi.org/10.1016/j.acra.2011.12.003.
[6] G. Andria, F. Attivissimo, G. Guglielmi, A.M.L. Lanzolla, A. Maiorana, M. Mangiantini, Towards patient dose optimization in digital radiography, Measurement 79 (2016) 331–338, https://doi.org/10.1016/j.measurement.2015.08.015.
[7] M. Uffmann, C. Schaefer-Prokop, Digital radiography: the balance between image quality and required radiation dose, Eur. J. Radiol. 72 (2009) 202–208, https://doi.org/10.1016/j.ejrad.2009.05.060.
[8] L. Martin, R. Ruddlesden, C. Makepeace, L. Robinson, T. Mistry, H. Starritt, Paediatric x-ray radiation dose reduction and image quality analysis, J. Radiol. Prot. 33 (2013) 621–633, https://doi.org/10.1088/0952-4746/33/3/621.
[9] G. Paulo, J. Santos, A. Moreira, F. Figueiredo, Transition from screen-film to computed radiography in a paediatric hospital: the missing link towards optimisation, Radiat. Prot. Dosimetry 147 (2011) 164–167, https://doi.org/10.1093/rpd/ncr355.
[10] H. Precht, O. Gerke, K. Rosendahl, A. Tingberg, D. Waaler, Large dose reduction by optimization of multifrequency processing software in digital radiography at follow-up examinations of the pediatric femur, Pediatr. Radiol. 44 (2014) 239–240, https://doi.org/10.1007/s00247-013-2854-3.
[11] P. Brosi, A. Stuessi, F. Verdun, P. Vock, R. Wolf, Copper filtration in pediatric digital X-ray imaging: its impact on image quality and dose, Radiol. Phys. Technol. 4

(2011) 148–155, https://doi.org/10.1007/s12194-011-0115-4.
[12] A. Almen, M. Lööf, S. Mattsson, Examination technique, image quality, and patient dose in paediatric radiology, Acta Radiol. 37 (1996) 337–342, https://doi.org/10.1177/02841851960371P171.
[13] C. Bloomfield, F. Boavida, D. Chabloz, E. Crausaz, E. Huizinga, H. Hustveite, H. Knighta, A. Pereirab, V. Harsakere, W. Schaaked, R. Visser, Experimental Article – Reducing Effective Dose to a Paediatric Phantom by Using Different Combinations of kVp, mAs and Additional Filtration Whilst Maintaining Image Quality, OPTIMAX 2014 – Radiation Dose and Image Quality Optimisation in Medical Imaging, Lisbon, Portugal, (2015).
[14] M. McEntee, P. Doherty, Optimisation of the pediatric pelvis radiographic examination, ECR 2011 (Poster No C-0265) (2011) 1–7, https://doi.org/10.1594/ecr2011/C-0265.
[15] M.-L. Butler, P. Brennan, Nonselective filters offer important dose-reducing potential in radiological examination of the paediatric pelvis, J. Med. Imaging Radiat. Sci. 40 (2009) 15–23, https://doi.org/10.1016/j.jmir.2008.11.002.
[16] E. Norrman, J. Persliden, A factorial experiment on image quality and radiation dose, Radiat. Prot. Dosimetry 114 (2005) 246–252, https://doi.org/10.1093/rpd/nch557.
[17] D. Montgomery, Design and Analysis of Experiments Eighth Edition, 8th ed., John Wiley & Sons, Inc., 2013.
[18] A. Mohammed Ali, P. Hogg, S. Johansen, A. England, Construction and validation of a low cost paediatric pelvis phantom, Eur. J. Radiol. 108 (2018) 84–91, https://doi.org/10.1016/j.ejrad.2018.09.015.
[19] F.E. Stieve, Radiological requirements for the specification of image quality criteria, Optim. Image Qual. Patient Expo. Diagn. Radiol. BIR Rep. 20 (1989) 221–238.
[20] M. Båth, M. Håkansson, J. Hansson, L.G. Månsson, A conceptual optimisation strategy for radiography in a digital environment, Radiat. Prot. Dosimetry 114 (2005) 230–235, https://doi.org/10.1093/rpd/nch567.
[21] M. Båth, Evaluating imaging systems: practical applications, Radiat. Prot. Dosimetry 139 (2010) 26–36, https://doi.org/10.1093/rpd/ncq007.
[22] J. Landis, G. Koch, The Measurement of Observer Agreement for Categorical Data Data for Categorical of Observer Agreement The Measurement 33 (1977), pp. 159–174.
[23] B. Rosner, Fundamentals of Biostatistics, 7th ed., Cengage Learning, Inc, 2010.
[24] Q. Carroll, Radiography in the Digital Age: Physics, Exposure, Radiation Biology, Charles C. Thomas, Springfield, Illinois, 2011.
[25] T. Fauber, Radiographic Imaging and Exposure, 4th ed., Elsevier Health Sciences, 2013.
[26] G. Alzen, G. Benz-Bohm, Radiation protection in pediatric radiology, Dtsch. Aerzteblatt Online 108 (2011) 407–414, https://doi.org/10.3238/arztebl.2011.0407.
[27] CIRS Tissue Simulation and Phantom Technology, ATOM® Dosimetry Phantoms: Models 701-706, (2011), p. 16 http://www.cirsinc.com/products/modality/33/atom-dosimetry-verification-phantoms/?details=resources.
[28] C.J. Martin, B. Farquhar, E. Stockdale, S. Macdonald, A study of the relationship between patient dose and size in paediatric radiology, Br. J. Radiol. (1994), https://doi.org/10.1259/0007-1285-67-801-864.
[29] V. Karami, M. Zabihzadeh, N. Shams, A. Gilavand, Optimization of radiological protection in pediatric patients undergoing common conventional radiological procedures: effectiveness of increasing the film to focus distance (FFD), Int. J. Pediatr. 5 (2017) 4771–4782, https://doi.org/10.22038/ijp.2017.22010.1841.
[30] P. Brennan, D. Johnston, Irish X-ray departments demonstrate varying levels of adherence to European guidelines on good radiographic technique, Br. J. Radiol. 75 (2002) 243–248, https://doi.org/10.1259/bjr.75.891.750243.
[31] R. Mooney, P.S. Thomas, Dose reduction in a paediatric X-ray department following optimization of radiographic technique, Br. J. Radiol. 71 (1998) 852–860, https://doi.org/10.1259/bjr.71.848.9828798.
[32] W.J.H. Veldkamp, L.J.M. Kroft, M.V. Boot, B.J.A. Mertens, J. Geleijns, Contrast-detail evaluation and dose assessment of eight digital chest radiography systems in clinical practice, Eur. Radiol. 16 (2006) 333–341, https://doi.org/10.1007/s00330-005-2887-6.
[33] C. Martin, C. Darragh, G. McKenzie, A. Bayliss, Implementation of a programme for reduction of radiographic doses and results achieved through increases in tube potential, Br. J. Radiol. 66 (1993) 228–233, https://doi.org/10.1259/0007-1285-66-783-228.
[34] P.-L. Khong, H. Ringertz, V. Donoghue, D. Frush, M. Rehani, K. Appelgate, R. Sanchez, ICRP publication 121: radiological protection in paediatric diagnostic and interventional radiology, Ann. ICRP 42 (2013) 1–63, https://doi.org/10.1016/j.icrp.2012.10.001.
[35] L. Lança, M. Bowdler, J. Creedon, V. Dayer, S. N, S. V.H, S. Pinhão, V. M.B, J.A. Pires Jorge, Paediatric Phantom Dose Optimization Using Digital Radiography with Paediatric Phantom Dose Optimisation Using Digital Radiography with Variation of Exposure Parameters and Filtration Whilst Minimising Image Quality Impairment, Optimax2018, 2018, pp. 77–92.
[36] J. Tugwell, C. Everton, A. Kingma, D.M. Oomkens, G.A. Pereira, D.B. Pimentinha, C.A.I. Rouiller, S.M. Stensrud, E. Kjelle, J. Jorge, P. Hogg, Increasing source to image distance for AP pelvis imaging – impact on radiation dose and image quality, Radiography 20 (2014) 351–355, https://doi.org/10.1016/j.radi.2014.05.012.
[37] H. Mraity, Optimisation of Radiation Dose and Image Quality for AP Pelvis Radiographic Examination, University of Salford, 2015.